

# Soft Matter

Accepted Manuscript



This is an *Accepted Manuscript*, which has been through the Royal Society of Chemistry peer review process and has been accepted for publication.

*Accepted Manuscripts* are published online shortly after acceptance, before technical editing, formatting and proof reading. Using this free service, authors can make their results available to the community, in citable form, before we publish the edited article. We will replace this *Accepted Manuscript* with the edited and formatted *Advance Article* as soon as it is available.

You can find more information about *Accepted Manuscripts* in the [Information for Authors](#).

Please note that technical editing may introduce minor changes to the text and/or graphics, which may alter content. The journal's standard [Terms & Conditions](#) and the [Ethical guidelines](#) still apply. In no event shall the Royal Society of Chemistry be held responsible for any errors or omissions in this *Accepted Manuscript* or any consequences arising from the use of any information it contains.

# Hydrodynamic Interaction Induced Spontaneous Rotation of Coupled Active Filaments

Huijun Jiang(江慧军) and Zhonghuai Hou(侯中怀)\*

*Department of Chemical Physics & Hefei National Laboratory for Physical Sciences at the Microscale,  
University of Science and Technology of China, Hefei, Anhui 230026, China*

(Dated: August 5, 2014)

We investigate coupled dynamics of active filaments with long range hydrodynamic interactions (HI). Remarkably, we find that filaments can rotate spontaneously in the same condition in which a single filament alone can only move in translation. Detailed analysis reveals that, the emergence of coupled rotation originates from asymmetric flow field associated with HI which breaks the symmetry of translation motion when filaments approach. The breaking then be further stabilized by HI to form self-sustained coupled rotation. Intensive simulations show that coupled rotation is easy to form when one filament tends to collide the front-half of the other. For head-to-tail approaching, we observe another interesting HI-induced coupled motion, where filaments move together in the form of one following up the other. What's more, the radius of coupled rotation increases exponentially as the rigidity of filament increases, which suggests that HI is also important for the alignment of rigid-rod-like filaments which has been assumed to be solely a consequence of direct collisions.

## I. INTRODUCTION

Active soft matter, a new and exciting class of complex system, has drawn great research attentions in very recent years[1, 2]. Such systems can be driven far from equilibrium by continuously consuming energy supplied internally or externally. One example is the cytoskeleton of eukariotic cells which consists of long filamentary proteins driven by molecular motors. Usually, the dynamics of filaments is governed by low Reynolds number hydrodynamics, where viscous effects dominate and inertial effects are negligible[3]. The dynamics also involves the active process by motor proteins walking on it which convert chemical energy into work and generate propulsions. Experiments of motility assays, where semiflexible filaments are driven to slide over a bed of motor proteins, reveal that active filaments can self-organize into fascinating coherently structures, such as asters, propagating density waves and vortexes [4–6]. A deep understanding of such collective patterns will shed light on not only the formation and stability of more complex structures of biological relevance, but also the mechanism of dynamic self-assembly associated with active soft matters in other disciplines.

Recently, two interesting experiments have investigated collective behaviors of active filaments with particular attention paid to the formation mechanism of vortexes[5, 6]. In the study of collective motion of actin filaments driven by meromyosin, the authors believed that hydrodynamic interaction (HI) is essential for the vortexes formation by comparing collective motions in experiments with those in cellular-automata simulations[5, 7]. On the other hand, Yutaka Sumino et al. argued that it is not HI but alignment of filaments and rotation curvature of a single filament that are necessary for the formation of vortexes [6], by investigating

the collective behavior of microtubes driven by dynein c. These two experiments thus presented a very attractive topic regarding how collective vortex structure emerges, especially the very role played by HI. Since vortex formation involves the motion of a single filament with intra-filament interactions and also the collective moving of multi-filaments with inter-filament interactions, HI may take effect at different scales, from the maintenance of rotation curvature at the single-filament level, to long range correlated motion involving multi-filaments.

At the single-filament level, it has been found that a bending instability of an initially straight filament spontaneously breaks flow symmetry and lead to autonomous filament motion[8], and the competition between the destabilising effect of HI induced by active force and the stabilising effect of elasticity provides a generic route to spontaneous oscillations in active filaments[9]. In a previous study, we have investigated thoroughly the dynamics of a single active filament, with particular attention paid to the role of intra-filament HI[10]. We showed that a single active filament may undergo successive motion transitions from translation to snaking and then to rotation with the changes of rigidity and driving force, and HI can significantly enlarge the parameter region where filament rotation occurs.

At the inter-filament level, HI may affect motion of filaments by inducing long-range interactions. Hitherto, there are many results and studies on the hydrodynamically coupled motion of both passive and active hard objects which shows no shape kinematics[11–24]. For example, HI may change the collective and relative diffusion of coupled passive objects remarkably[11–15], and once the particle are under activity, a transition from diffusive to ballistic motion can be observed[17]. Besides the fundamental statistics of Brownian fluctuations, it is now understood that this coupling is also important to dynamics at time scales relevant to biological systems[16] and colloidal systems[18, 19]. For particles with activity or driven by external force, variety new types of dynamics may be formed[20]. It is found that, self-coupling of

---

\*Electronic address: hzh1j@ustc.edu.cn

translation and rotation of one trapped sphere can be induced by HI of the neighboring one[21, 22]. Recently, synchronization of oscillation by hydrodynamic coupling has been observed for several systems[23, 24]. However, to our best knowledge, the effect of HI on coupled dynamics of semiflexible filaments with shape kinematics is still unexplained. It is thus merited and very desired to investigate the coupled dynamics of such active filaments.

In the present paper, we investigate the motion of two coupled active filaments with both intra- and inter-filament HI. We show that HI plays a crucial role for the emergence of coupled motions by inducing asymmetric flow fields around each filament, which further enforces changes on the shape kinematics of the filaments. In the parameter region where a single filament can only move in translation, such a flow-enforced change may break the stability of the translation motion, leading to an interesting type of coupled rotation (CR), which is further stabilized by the HI. By extensive simulations, we show that such a CR behavior can easily be observed when the two filaments approach in a head-to-front manner, i.e., the head of one filament tends to collide with the front half of the other one. Furthermore, we find that the radius of CR grows exponentially with the filament rigidity, indicating that HI can also result in alignment of rigid-rod-like filaments. Other interesting type of coupled motions can also be observed, for instance, a filament may follow up closely the trajectory of the other one when the former approaches the latter in a head-to-tail manner.

## II. MODEL AND METHOD

As shown in Fig.1(a), our simulation is based on the same bead-rod model consisting of  $N$  beads connected by  $N - 1$  inextensible rods as in our previous paper[10]. The time evolution of the bead positions  $\mathbf{r}_i(\tau)$  is governed by the following over-damped Langevin equation

$$\dot{\mathbf{r}}_i(\tau) = \sum_{j=1}^N \mu_{ij}(\mathbf{r}_{ij}) \left[ \mathbf{F}_j^{sp,b} + \mathbf{F}_j^{dr,b} - \frac{\partial U(\{\mathbf{r}_i\})}{\partial \mathbf{r}_j} \right] + \zeta_i(\tau). \quad (1)$$

Herein, the interaction potential  $U(\{\mathbf{r}_i\})$  includes a bending part  $U^B = \frac{1}{2} \left(\frac{\kappa}{\pi}\right) \beta_i^2$  which tends to keep the angle  $\beta_i$  between adjacent rod vectors close to its equilibrium value of zero, and a truncated Lennard-Jones (LJ) potential  $U^{LJ}(r_{ij}) = 4\xi \left\{ (2a/r_{ij})^{12} - (2a/r_{ij})^6 \right\} + \xi$  which accounts for the exclusive volume effect.  $r_{ij}$  denotes the distance between beads  $i$  and  $j$ . The parameter  $\kappa$  measures the filament rigidity,  $\xi$  measures the LJ-coupling strength, and the repulsive distance between beads is given by  $2\sqrt[6]{2}a$ .

HI between two different beads is implemented via the Ronte-Prager-Yamakawa mobility tensor  $\mu_{ij}$  [25, 26].

When  $i \neq j$ ,

$$\mu_{ij} = \mu_0 \left[ \frac{3a}{4r_{ij}} (\mathbf{1} + \hat{\mathbf{r}}_{ij}\hat{\mathbf{r}}_{ij}) + \frac{a^3}{2r_{ij}^3} (\mathbf{1} - 3\hat{\mathbf{r}}_{ij}\hat{\mathbf{r}}_{ij}) \right], \quad (r \geq 2a) \quad (2a)$$

$$\mu_{ij} = \mu_0 \left[ \left(1 - \frac{9}{32} \frac{r_{ij}}{a}\right) \mathbf{1} + \frac{3}{32} \frac{r_{ij}\hat{\mathbf{r}}_{ij}\hat{\mathbf{r}}_{ij}}{a} \right]. \quad (r \leq 2a) \quad (2b)$$

$\mathbf{1}$  denotes the three-dimensional unit matrix and  $\hat{\mathbf{r}}_{ij}\hat{\mathbf{r}}_{ij}$  is the outer product of the normalized vectors  $\hat{\mathbf{r}}_{ij} = \mathbf{r}_{ij}/r_{ij}$ . The self-mobility of bead  $i$  is given by  $\mu_{ii} = \mu_0 \mathbf{1}$  with  $\mu_0 = 1/(6\pi\eta a)$  and  $\eta$  the viscosity of the aqueous solvent.  $\zeta(t)$  models the random force from the heat bath and obeys the fluctuation-dissipation theorem  $\langle \zeta_i(\tau)\zeta_j(\tau') \rangle = 2k_B T_0 \mu_{ij} \delta(\tau - \tau')$  with  $k_B$  the Boltzmann constant and  $T_0$  the temperature.

The rigid constraints (rod) between adjacent beads are realized by FENE-Fraenkel (FF) springs [27], and the force exerted on bead  $i$ ,  $\mathbf{F}_i^{sp,b} = \mathbf{F}^{sp}(\mathbf{v}_i) - \mathbf{F}^{sp}(\mathbf{v}_{i-1})$  ( $\mathbf{v}_i = \mathbf{r}_{i+1} - \mathbf{r}_i$ ), is obtained via summation over the two adjacent FF-springs.

$$\mathbf{F}^{sp}(\mathbf{v}) = \frac{H(|\mathbf{v}| - r_0)}{1 - (|\mathbf{v}| - r_0)^2 / (r_0 \delta)^2} \frac{\mathbf{v}}{|\mathbf{v}|}, \quad (1 - \delta) < \frac{|\mathbf{v}|}{r_0} < (1 + \delta). \quad (3)$$

where  $r_0$  is the rod length and  $\delta$  is the maximal extension allowed.

By assuming homogeneous distribution of motors on the surface, it is reasonable to suggest that the active force on unit length of the filament can be viewed as a constant, i.e., each bond is subject to a constant force  $\alpha$  along its direction. Accordingly, the active force on bead  $i$  is then also a summation over the two adjacent filament segments,  $\mathbf{F}_i^{dr,b} = \alpha(\mathbf{v}_i/|\mathbf{v}_i| + \mathbf{v}_{i-1}/|\mathbf{v}_{i-1}|)$ . Since the filament is mainly confined in a plane, the model we proposed here actually describes a two-dimensional dynamics with three-dimensional hydrodynamics.

In simulations, Eq.(1) is discretized with time step  $\Delta$ , and an implicit predictor-corrector method is employed to realize the rod-length constraint as described in detail in [27]. The length, time and energy are rescaled by the bead diameter  $2a$ , the time step  $\Delta$  and the energy parameter of Lennard-Jones potential  $\xi$ , respectively, and thus the dimensionless self-mobility is  $\tilde{\mu}_0 = \mu_0 \xi \Delta / (2a)^2$ . Other parameters are  $k_B T_0 = \xi / 100$ ,  $N = 10$ , filament length  $L / (2a) = 18$  (and a consequent rod length  $r_0 / (2a) = 2$ ),  $\delta = 0.02$ , rigidity  $\kappa / 10^3 = 10$  and active force  $\alpha / 10^3 = 4$  if not otherwise stated.

## III. RESULT

To begin, we investigate how two filaments move when they encounter each other with or without HI. The parameters above are chosen such that a single filament only shows translation motion in a certain speed according to our previous results[10]. When two filaments are far away from each other, they will just move along their

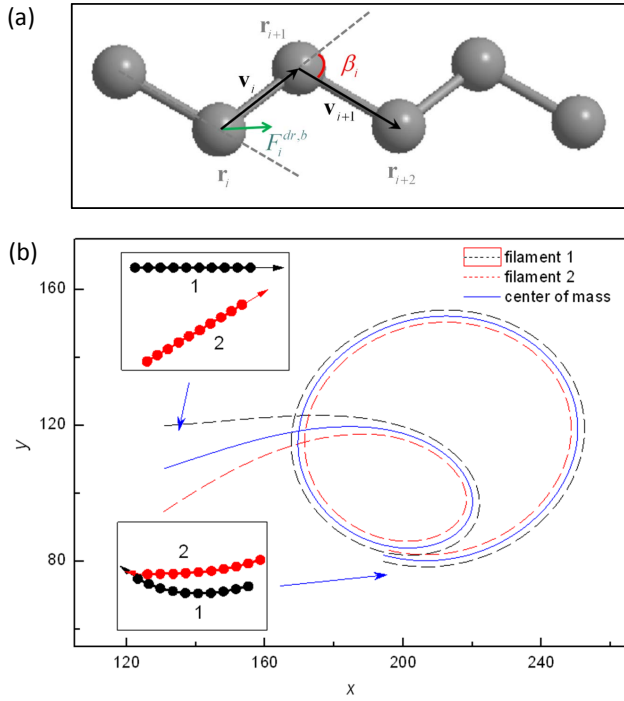


FIG. 1: (a) Bead-rod model of the active filament. (b) Spontaneous rotation of coupled active filaments in the parameter region where a single filament can only move translationally. The top-left and bottom-left insets show typical configurations of filaments before and in rotation, respectively.

initial directions as shown in the top-left inset of Fig.1. However, when these two filaments move close enough to each other, they will tie together and show sustained CR spontaneously. This is demonstrated by the trajectories of the two filaments as well as their center of mass (CM) in Fig.1, where they change from initial straight lines to repeated cycles asymptotically. Surely this cannot be the result of simple collision, and reveals new feature associated with filament coupling.

The distance between the two filaments,  $D$ , is used as an order parameter to quantitatively describe the collision process,

$$D = |\mathbf{r}_{cm,1} - \mathbf{r}_{cm,2}|, \quad (4)$$

where  $\mathbf{r}_{cm,i} = (1/N) \sum_{j \in \text{filament } i} \mathbf{r}_j$ . Clearly, as shown in Fig.2(a),  $D$  decreases as the two filaments approach and then keeps a certain small value after collision, which indicates that the two filaments are moving in a coupled way. The motion of filaments after collision is quantified by the power spectrum of the trajectories of the CM. In Fig.2(b), clear-cut peaks provide a further evidence for that a CR motion is formed after the collision of two active filaments. The value of the first peak is about  $4.69 \times 10^{-5}$ , corresponding to the rotation period of CR,  $2.13 \times 10^4$  time steps.

To show comparison, the order parameter  $D$  and pow-

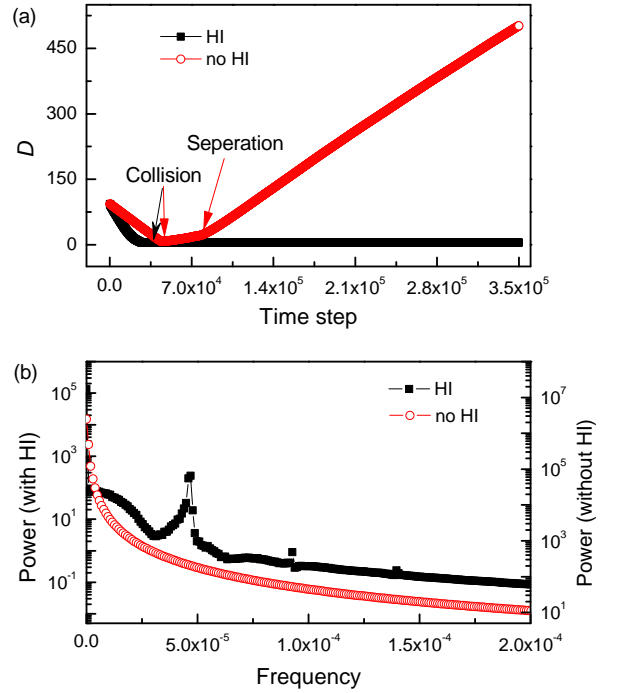


FIG. 2: Comparison of collision dynamics with and without hydrodynamic interaction. (a) Time evolution of order parameter  $D$  (the distance between the two filaments) and (b) power spectrums of the trajectories of the CM (center of mass).

er spectrum for the collision of active filaments without HI are also plotted in Fig.2(a) and (b), respectively. In this case, both filaments move separately along straight lines at first. When collision happens, they change to coupled translation, and  $D$  starts to increase linearly with a smaller slope. Such coupled translation motion is not stable and shortly after the two filaments separate again. Once they are decoupled,  $D$  grows linearly with a larger slope as time increases, which is simply due to the fact that the filaments move translationally in a certain speed. The power spectrum also demonstrates that there is no CR formed after the collision without HI. The above distinguished differences between the observations with and without HI evidently demonstrate that HI plays an important role in coupled dynamics of active filaments. Specifically, HI can induce spontaneous CR although a single filament alone can only move translationally.

According to Fig.1, the two filaments start to rotate at a distance rather larger than the range of direct collision. At this distance, the dominated correlation between the two filaments is the long range HI. Therefore, it is instructive to investigate the flow field generated by the filaments and how it would influence the filament motion. According to Eq.(1), a force  $\mathbf{F}_s$  on a bead located at  $\mathbf{r}_s$  will result in a drift  $\mathbf{v}_s(\mathbf{r}_t) = \mu_{t,s}(\mathbf{r}_{t,s})\mathbf{F}_s$  at location  $\mathbf{r}_t$ , and hence the flow field induced by a single filament  $i$  (assuming no other filaments exists) can be obtained as  $\mathbf{V}_i(\mathbf{r}_t) = \sum_{s \in i} \mathbf{v}_s(\mathbf{r}_t)$ . In Fig.3(a), we have plotted the flow field  $\mathbf{V}_1(\mathbf{r}_t)$  generated by a filament (we may

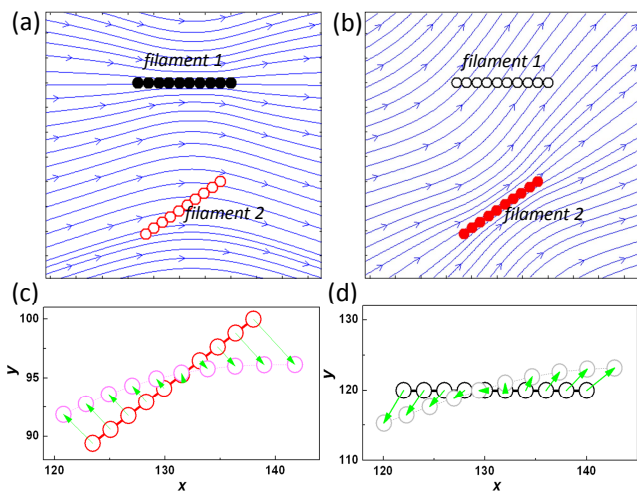


FIG. 3: Hydrodynamic interaction induced asymmetric flow field associated with (a) filament 1 (the top one, indicated by solid black cycles) and (b) filament 2 (the bottom one, indicated by solid red cycles), and the resulting bending tendency on the shape of (c) filament 2 and (d) filament 1. In (c) and (d), the green arrow represents relative moving tendency of each bead to the center of mass, which has been magnified  $10^4$  times.

name it as filament 1) moving horizontally to the right, which is obviously not homogeneous. Note that this field generated by filament 1 itself will not influence its shape kinematics, i.e., filament 1 will keep its translational motion. However, when a second filament 2 comes nearby as indicated by the open symbols in Fig.3(a), this field  $\mathbf{V}_1(\mathbf{r}_t)$  will enforce additional drift on it. As a result, the velocity of CM of filament 2 may change, and more importantly, the drifts on different beads will be different due to the asymmetry of the flow field around filament 2, which may break the stability of its translation motion. To make this more clearly, the relative drifts of each bead of filament 2 to its CM are presented in Fig.3(c) (indicated by green arrows), where the expected configuration is also plotted to show how its shape kinematics changes as a consequence of the enforced drifts. Such a bending tendency is favorable both for the alignment of the two filaments and for the rotation of filament 2. In a similar way, filament 2 can also induce an asymmetric flow field around filament 1 as shown in Fig.3(b), which will also lead to bending of filament 1 toward alignment with filament 2. Consequently, both filaments bend toward alignment with each other and rotate in the same direction. In short, when the two filaments approach in an appropriate way as shown in Fig.1, HI will induce loss-of-stability of translation motion of both filaments and CR can emerge.

Once the CR starts, another important factor is about its stability for maintenance of the curvature. To elucidate such a point, we have plotted the total flow field  $\sum_{i=1}^2 \mathbf{V}_i(\mathbf{r}_t)$  induced by both filaments in Fig.4(a) for a typical configuration. As can be seen, there exists a slight vortex near the front of the two filaments resulting from

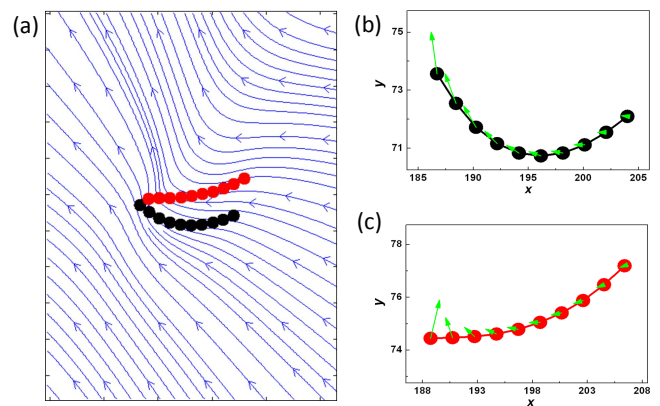


FIG. 4: Self-sustained rotation motion of coupled filaments with the help of hydrodynamic interaction. (a) Hydrodynamic interaction induced total flow field, and the resulting drifts (indicated by green arrows) on (b) filament 1 and (c) filament 2. Notice that, the drifts have been magnified  $10^2$  times.

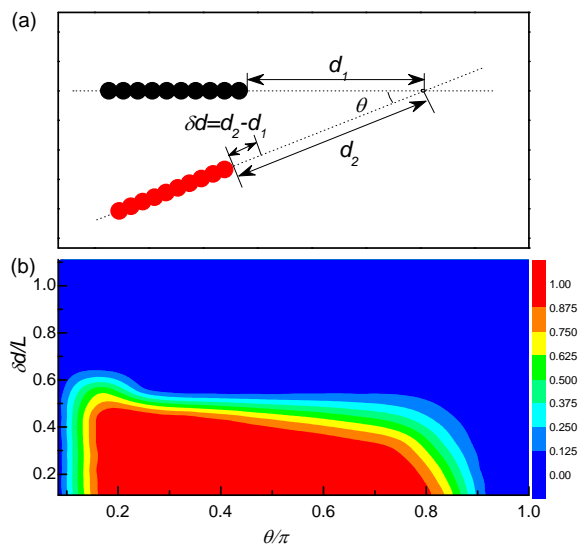


FIG. 5: (a) Schematic diagram for the definition of initial condition parameters, collision angle  $\theta$  and relative position  $\delta d$ . (b) Probability of rotation formation in the  $\theta - \delta d$  plane. For  $M_0$  times simulation starting with given  $\theta$  and  $\delta d$ , the probability is defined as  $M/M_0$ , where  $M$  is the number of simulations in which CR of active filaments is formed.

the bending shapes and the active forces. Consequently, the flow field provides vortex drifts to both filament 1 and filament 2 in return, as shown in Fig.4(b) and (c), which keeps the bending shape of each filament as well as their CR. In other words, HI can also ensure the stability of the CR after it has been formed.

The results above are obtained by considering the specific initial condition as shown in Fig.1. To be more general, one needs to understand how the observed CR

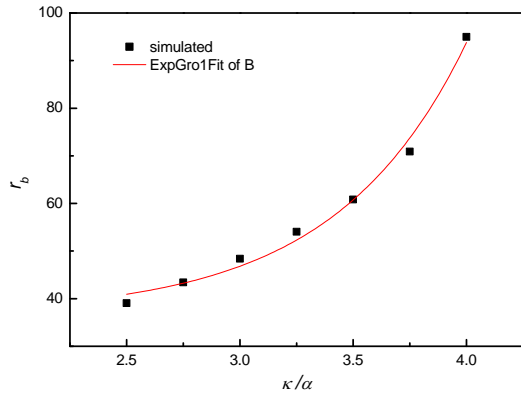


FIG. 6: The radius of rotation curvature  $r_b$  as a function of the ratio of rigidity and active force  $\kappa/\alpha$  with fixed collision angle  $\theta = 0.2\pi$  and relative position  $\delta d/L = 0.1$ . The simulated result can be well fitted by a growing exponential function  $r_b = Ae^{B\kappa/\alpha} + r_0$  with  $B = 1.73$ .

depends on the choice of initial conditions. Since each filament alone moves translationally, we can define two parameters to quantify the initial condition as shown in Fig.5(a): The collision angle  $\theta$  and the relative position denoted by  $\delta d$ . Note that if  $\delta d < L/2$ , we say that the two filaments collide in a 'head-to-front' manner. Since the dynamics is stochastic, the final motion of the two filaments may depend on  $\theta$  and  $\delta d$  in a probabilistic way. We thus run totally  $M_0$  times of simulations with the same  $(\theta, \delta d)$  and record the times  $M$  when CR happens, and then calculate the probability  $p(\theta, \delta d)$  via  $M/M_0$ . The contour plot of  $p(\theta, \delta d)$  for various  $\theta$  and  $\delta d$  is plotted in Fig.5(b). Interestingly, the CR motion can be observed for a wide range of collision angle  $\theta$  once  $\delta d/L < 0.5$ , i.e., the filaments collide in the 'head-to-front' manner mentioned above. In addition,  $p(\theta, \delta d) \approx 1$  is not sensitive to  $\theta$  indicating that CR is a rather robust phenomenon, except for  $\theta$  close to 0 or  $\pi$  where the two filaments are nearly (anti-)parallel. We will show later that in parallel situations, another interesting type of coupled motion can be observed.

We have also investigated how the rigidity of filament and active force affect the rotation which can be reduced in to a dimensionless parameter  $\kappa/\alpha$ . For fixed  $\theta = 0.2\pi$  and  $\delta d/L = 0.1$  where CR can always be observed, the radius of the rotation trajectory  $r_b$  as a function of  $\kappa/\alpha$  is plotted in Fig.6. One sees that more rigid filaments (or less active force) show CR motion with larger radius. Moreover, the dependence of  $r_b$  on  $\kappa/\alpha$  can be well fitted by a growing exponential function  $r_b = Ae^{B\kappa/\alpha} + r_0$  with  $B \simeq 1.73$ . This implies that the radius of CR motion for two coupled relative hard filaments ( $\kappa/\alpha \rightarrow \infty$ ) tends to infinity, i.e., they essentially move together with parallel alignment in the same direction. Recall that the two filaments will finally separate apart in the absence of HI as already shown in Fig.2, therefore, our results suggest that HI could be important mechanism for alignment of rigid-rod-like filaments which has been assumed to be

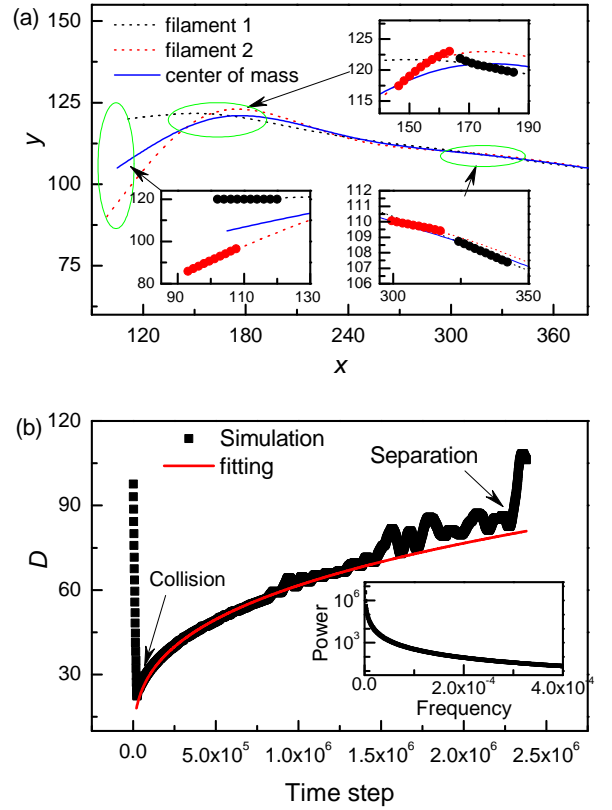


FIG. 7: Following-up motion of coupled active filaments when they approach each other longitudinally. (a) Trajectories of the two filaments and their CM. The bottom-left inset shows the initial configuration of filaments with collision angle  $\theta = 0.2\pi$  and relative position  $\delta d = 1.2L$ . Typical configurations during and after the formation of following motion are presented in insets at top-right and bottom-right, respectively. (b) The order parameter  $D$  as a function of simulation time. For a long time period after collision, the simulation result can be well fitted by  $D = c_1 \cdot (\text{Time step})^{c_2}$  with  $c_1 = 0.805$  and exponent  $c_2 = 0.314$ . The inset shows the power spectrum of the following-up trajectory.

solely a consequence of direct collisions [6].

As pointed out above, other interesting types of coupled motion may occur besides CR. Specifically, when filament 2 approaches filament 1 in a head-to-tail way, they may move together in a form that one filament following the other. As an example, the whole approaching process with  $\theta = 0.2\pi$  and  $\delta d = 1.2L$  is shown in Fig.7. The moving directions of both filaments adjust to the same one after a short relaxation of coupled motion when they encounter each other. Note that this motion is quite different from conventional alignment process where two rigid-rod-like filaments move side by side [6]. Typical configurations during and after the formation of following-up motion are presented in the insets at top-right and bottom-right of Fig.7(a), respectively. Since there is no direct collision during the formation process, which can be seen by taking a closer look at the configuration of filaments in the top-right inset in

Fig.7(a), this type of following-up motion could also be induced by long range HI. This conclusion can be further verified by the time evolution of order parameter  $D$  as shown in Fig.7(b). It is quite interesting that, for a long time period after collision,  $D$  can be well fitted by  $D = c_1 \cdot (\text{Time step})^{c_2}$  with  $c_1 = 0.805$  and exponent  $c_2 = 0.314$ . Notice that, the small value of  $c_1$  suggests a slower growth of  $D$  than the linear one for two filaments without HI (as observed in Fig.2(a)), implying that HI does play an important role for coupled filament motion.

#### IV. CONCLUSION

In conclusion, coupled dynamics of semiflexible active filaments has been studied with both intra- and inter-filament HI. This research revealed that HI is crucial for coupled motion by enforcing additional changes on shape kinematics of filaments, which can induce coupled rotation for 'head-to-front' filaments and following-up motion for 'head-to-tail' filaments. Wherein, the asymmet-

ric flow field resulting from HI breaks the symmetry of translation in the parameter region where a single filament can only move in translation, and further stabilizes the breaking to form self-sustained coupled rotations. We also demonstrate that alignment of rigid-rod-like may not simply originate from direct collision, but also from HI. These findings provide a deep understanding of coupled dynamics of active filament and the complex role of HI played, which takes an important step forward to underlying mechanism of collective behaviors observed in experiments. We hope that the present study could draw more theoretical research interests and open new perspectives on the study of collective motion in active systems.

#### Acknowledgments

This work is supported by National Science Foundation of China(91027012, 21125313) and National Basic Research Program of China (2013CB834606).

- 
- [1] M. C. Marchetti, J. F. Joanny, S. Ramaswamy, T. B. Liverpool, J. Prost, M. Rao, and R. A. Simha, *Rev. Mod. Phys.* **85**, 1143 (2013).
  - [2] F. C. MacKintosh and M. E. Cates, *Soft Matter* **7**, 3050 (2011).
  - [3] J. Happel and H. Brenner, *Low Reynolds Number Hydrodynamics* (Prentice-Hall, Englewood Cliffs, NJ, 1965).
  - [4] F. J. Nedelec, T. Surrey, A. C. Maggs, and S. Leibler, *Nature* **389**, 305 (1997).
  - [5] V. Schaler, C. Weber, C. Semmrich, E. Frey, and A. R. Bausch, *Nature* **467**, 73 (2010).
  - [6] Y. Sumino, K. H. Nagai, Y. Shitaka, D. Tanaka, K. Yoshikawa, H. Chaté, and K. Oiwa, *Nature* **483**, 448 (2012).
  - [7] V. Schaler, C. Weber, E. Frey, and A. R. Bausch, *Soft Matter* **7**, 3213 (2011).
  - [8] G. Jayaraman, S. Ramachandran, S. Ghose, A. Laskar, M. S. Bhamla, P. S. Kumar, and R. Adhikari, *Phys. Rev. Lett.* **109**, 158302 (2012).
  - [9] A. Laskar, R. Singh, S. Ghose, G. Jayaraman, P. S. Kumar, and R. Adhikari, *Scientific Reports* **3**, 1964 (2013).
  - [10] H. Jiang and Z. Hou, *Soft Matter* **10**, 1012 (2014).
  - [11] T. G. M. van de Ven, *Colloidal Hydrodynamics* (Academic Press, San Diego, 1989).
  - [12] P. N. Segre, E. Herbolzheimer, and P. M. Chaikin, *Phys. Rev. Lett.* **79**, 2574 (1997).
  - [13] J.-C. Meiners and S. R. Quake, *Phys. Rev. Lett.* **82**, 2211 (1999).
  - [14] B. Lin, B. Cui, J. Lee, and J. Yu, *Europhysics Letters* **57**, 724 (2002).
  - [15] X. Xu, S. A. Rice, B. Lin, and H. Diamant, *Phys. Rev. Lett.* **95**, 158301 (2005).
  - [16] D. A. Beard and T. Schlick, *J. Chem. Phys.* **112**, 7323 (2000).
  - [17] A. Vilfan and F. Julicher, *Phys. Rev. Lett.* **96**, 058102 (2006).
  - [18] G. Nagele and P. Baur, *Physica A* **245**, 297 (1997).
  - [19] D. Roehm, S. Kesselheim, and A. Arnold, *Soft Matter* **10**, 5503 (2014).
  - [20] I. Llopis and I. Pagonabarraga, *Europhysics Letters* **75**, 999 (2006).
  - [21] M. Reichert and H. Stark, *Phys. Rev. E* **69**, 031407 (2004).
  - [22] S. Martin, H. Stark, and T. Gisler, *Phys. Rev. Lett.* **97**, 248301 (2006).
  - [23] J. Kotar, M. Leoni, B. Bassetti, M. C. Lagomarsino, and P. Cicuta, *Europhysics Letters* **107**, 7669 (2010).
  - [24] J. Elgeti, U. Kaupp, and G. Gompper, *Biophys. J.* **99**, 1018 (2010).
  - [25] J. Rotne and S. Prager, *J. Chem. Phys.* **50**, 4831 (1969).
  - [26] H. Yamakawa, *J. Chem. Phys.* **53**, 436 (1970).
  - [27] C.-C. Hsieh, L. Li, and R. G. Larson, *Non-Newtonian Fluid Mech.* **112**, 141 (2003).